Lorentz-Violating Dynamics

Jesse Thaler

March 5, 2004 / March 12, 2004

1 Ghost Condensation and Standard Model Dynamics

We have seen that the theory of ghost condensation [1] is the universal low-energy effective theory coming from spontaneous time diffeomorphism breaking [2]. This theory offers unique insight into Lorentz- and CPT-violating effects that are not present in models with simple soft breaking terms, because the perturbations around the ghost vacuum are a *physical* excitation. Therefore, ghost condensation is not only a Lorentz-violating theory but also one with interesting dynamical properties.

In particular, we might imagine that the Goldstone boson π associated with the broken time diffeomorphism symmetry could couple directly to Standard Model fields. The most interesting coupling — and probably the most dangerous coupling phenomenologically — is a coupling to fermion spin-densities. We will see that this leads to two very interesting effects. First, a point-like spin moving with respect to the ghost vacuum with radiate away energy à la Cherenkov radiation until it is at rest relative to the ghost vacuum. Second, the π field can mediate a long-range force between spins with an interesting velocity dependence.

In essence, the theory of ghost condensation is the consistent effective field theory of the ether. While there are tight experimental bounds on possible soft Lorentz-violating terms, there are fewer bounds on dynamical Lorentz-violations, because most other "ether" models assume that the mediating bosons have the usual $w \sim k$ dispersion relation. But the excitations of the ghost ether have a novel dispersion relation that lead to novel dynamics, revealing new physics in a completely consistent framework.

2 Allowed Couplings to Standard Model Fields

We can easily generate all potential couplings between the π field and Standard Model fields by using the Higgs-like language of ghost condensation [1]. In that language, a scaler field ϕ picks up a vacuum expectation value

$$\langle \phi \rangle = M^2 t + \pi, \tag{1}$$

where M is the scale of spontaneous time diffeomorphism breaking, and π is the excitation around the ghost vacuum. We are working in a coordinate system that is at rest relative to $\langle\dot{\phi}\rangle$. Before ϕ picks up a vev, the ghost Lagrangian has a shift symmetry $\phi \to \phi + a$, so ϕ must couple derivatively. Therefore, we can generate all possible interactions by forming all Lorentz-invariant operators involving $\partial_\mu \phi$ and then expanding ϕ around its vacuum expectation value.

The leading Lorentz-invariant coupling of ϕ to Standard Model fermions is

$$\mathcal{L}_{\rm int} = \sum_\psi \frac{c_\psi}{F} \bar{\psi}\bar{\sigma}^\mu \psi \partial_\mu \phi, \tag{2}$$

where F is some mass scale. We can actually remove these couplings via a field redefinition

$$\psi \to e^{ic_\psi \phi/F}\psi, \tag{3}$$

but if there are Dirac mass terms in the action that break the $U(1)$ symmetry $\psi \to e^{i\theta}\psi$, $\psi_c \to e^{i\theta}\psi_c$, then the coupling to the fermion vector current can be removed but the coupling to the fermion axial current remain. In particular, we are left with

$$\mathcal{L}_{\rm int} = \frac{c_\Psi}{F}\bar{\Psi}\gamma^\mu\gamma^5\Psi\partial_\mu\phi. \tag{4}$$

Expanding around the ϕ vacuum $\langle\phi\rangle = M^2 t + \pi$,

$$\mathcal{L}_{\rm int} = \frac{c_\Psi}{F}\left(M^2\bar{\Psi}\gamma^0\gamma^5\Psi + \bar{\Psi}\gamma^0\gamma^5\Psi\dot{\pi} + \bar{\Psi}\vec{\gamma}\gamma^5\Psi\cdot\vec{\nabla}\pi\right). \tag{5}$$

The first term gives rise to different dispersion relations for particles and anti-particles. The second term can be removed by introducing interactions of higher order in $\partial_\mu\phi$ [2]. The last term gives us the interesting Lorentz-violating dynamics.

In the non-relativistic limit, the quantity $\bar{\Psi}\vec{\gamma}\gamma^5\Psi$ is the fermion spin-density $\vec{s}$ [3]. Therefore, we have a coupling between spin-density and the π field

$$\mathcal{L}_{\rm int} \sim \frac{1}{F}\vec{s}\cdot\vec{\nabla}\pi. \tag{6}$$

Note that this particular coupling can be forbidden by assuming a $\phi \to -\phi$ symmetry (or a time reversal invariance on the π theory coupled to gravity), but in general we expect that some coupling of a 3-vector to $\vec{\nabla}\pi$ will be generated through graviton loops. If $\mathcal{O}^{\mu\nu}$ is a dimension four Standard Model operator, then there is no symmetry forbidding the coupling

$$\mathcal{L}_{\rm int} \sim \frac{1}{M_{\rm Pl}^4}\mathcal{O}^{\mu\nu}\partial_\mu\phi\partial_\nu\phi \to \frac{M^2}{M_{\rm Pl}^4}\mathcal{O}^{0i}\partial_i\pi. \tag{7}$$

One interesting candidate for $\mathcal{O}^{\mu\nu}$ is the stress-energy tensor $T^{\mu\nu}$, and T^{0i} is just the total momentum density. Therefore, our analysis for spin-densities will carry over nicely for other 3-vector densities, albeit with different coupling constants.

3 Ether Cherenkov Radiation

In classical electrodynamics, Cherenkov radiation occurs when a charged particle moves through a medium at velocities higher than the speed of light in that medium. It can be thought of as the optical analog of a sonic boom. By energy conservation, the charged particle must lose energy in order to generate the photonic shockwave, and once the particle's velocity is less than the medium's light speed, the Cherenkov radiation ceases.

In the case of the ghost condensate, the dispersion relation for the π field is

$$w \sim \frac{k^2}{M}, \tag{8}$$

where M is the scale of spontaneous time diffeomorphism breaking. The velocity for the π field is

$$v \sim \frac{w}{k} = \frac{k}{M}, \tag{9}$$

so for a particle traveling at some fixed velocity v_0, there is always a k such that the speed of π is less than the speed of the particle. Therefore, we expect that a particle in motion relative to the ether — and which couples to the π field — will radiate away energy until it is at rest with respect to the ether.

In the case of usual Cherenkov radiation, we can use photon detectors to study the photonic shockwave and use that information to understand the motion of the charged particles. A variation of this idea is used in neutrino detectors like Super-K. Unfortunately, we don't (yet) have π field detectors, so the most likely experimental signature of ether Cherenkov radiation would be slight, unexplained kinetic energy loss for particles with spin. (More precisely, kinetic energy *gain* in the reference frame moving with respect to the ether.)

We can use a trick to calculate dE/dt for the particle in motion (*i.e.* the amount of power needed to maintain the particle kinetic energy despite the ether drag). The Lagrangian for the π field coupled to a spin-density source is

$$\mathcal{L} = \frac{1}{2}\dot{\pi}^2 - \frac{1}{2M^2}(\nabla^2\pi)^2 + \frac{1}{F}\vec{s}\cdot\vec{\nabla}\pi. \tag{10}$$

The equation of motion for the π field is

$$\ddot{\pi} + \frac{1}{M^2}\nabla^4\pi = -\frac{1}{F}\vec{\nabla}\cdot\vec{s}. \tag{11}$$

Multiplying both sides by $\dot{\pi}$, integrating over all space, and rewriting:

$$\frac{d}{dt}\left(\int d^3r\ \frac{1}{2}\dot{\pi}^2 + \frac{1}{2M^2}(\nabla^2\pi)^2\right) = \frac{1}{F}\int d^3r\ \vec{s}\cdot\vec{\nabla}\dot{\pi}. \tag{12}$$

We recognize the term in parenthesis as the energy of the π field. Any energy that goes into the π field is energy that we would need to pump into the moving spin to maintain it's velocity relative to the ether. Therefore, the rate of energy loss by the moving spin due to ether Cherenkov radiation is

$$\frac{dE_{\text{spin}}}{dt} = -\frac{1}{F}\int d^3r\ \vec{s}\cdot\vec{\nabla}\dot{\pi}. \tag{13}$$

We can calculate this energy dissipation for a spin-density corresponding to a point-like spin moving with velocity $\vec{v}$ relative to the ether:

$$\vec{s} = \vec{S}\, \delta^{(3)}(\vec{r} - \vec{v}t). \tag{14}$$

Plugging this into our energy dissipation equation

$$\frac{dE_{\text{spin}}}{dt} = -\frac{1}{F}\vec{S} \cdot \vec{\nabla}\dot{\pi}(\vec{v}t, t) \tag{15}$$

Using the Green's function for the π field, we can calculate the field π due to the source $\vec{s}$. In momentum space, the source looks like

$$\tilde{\vec{s}} = (2\pi)\vec{S}\, \delta(w - \vec{k} \cdot \vec{v}), \tag{16}$$

and the π field like

$$\tilde{\pi} = \frac{2\pi}{F} \frac{-i\vec{k} \cdot \vec{S}}{w^2 - k^4/M^2} \delta(w - \vec{k} \cdot \vec{v}). \tag{17}$$

Going back to position space,

$$\begin{aligned} \frac{1}{F}\vec{S} \cdot \vec{\nabla}\dot{\pi}(\vec{v}t, t) &= \frac{1}{F^2} \int \frac{d^3k\, dw}{(2\pi)^3} \frac{(-i\vec{k} \cdot \vec{S})(i\vec{S} \cdot \vec{k})(-iw)}{w^2 - k^4/M^2} \delta(w - \vec{k} \cdot \vec{v}) e^{-iwt} e^{i\vec{k}\cdot\vec{v}t} \\ &= \frac{-i}{F^2} \int \frac{d^3k}{(2\pi)^3} \frac{(\vec{S} \cdot \vec{k})^2 (\vec{k} \cdot \vec{v})}{(\vec{k} \cdot \vec{v})^2 - k^4/M^2} e^{-i\vec{k}\cdot\vec{v}t} e^{i\vec{k}\cdot\vec{v}t} \\ &= \frac{-iM^2}{F^2} \int \frac{k^2 dk\, d\Omega}{(2\pi)^3} \frac{k^3}{k^2} \frac{(\vec{S} \cdot \hat{k})^2 (\hat{k} \cdot \vec{v})}{(M\hat{k} \cdot \vec{v})^2 - k^2}. \end{aligned} \tag{18}$$

We can do the k integral by noting that there are poles at $k = \pm M\hat{k} \cdot \vec{v}$. We choose an $i\epsilon$ pole prescription such that our moving particle loses rather than gains energy.

$$\begin{aligned} \frac{dE_{\text{spin}}}{dt} &= -\frac{M^4}{4F^2} \int \frac{d\Omega}{(2\pi)^2} (\vec{S} \cdot \hat{k})^2 |\vec{v} \cdot \hat{k}|^3 \\ &= -\frac{M^4}{F^2} \frac{|v|}{96\pi} \left(|S|^2 |v|^2 + 3(\vec{S} \cdot \vec{v})^2 \right) \end{aligned} \tag{19}$$

We see that the rate of energy loss is roughly proportional to v^3. (By the way, you probably shouldn't trust the factor of 96π. The other factors should be correct, though.)

We can follow the same logic for a "spin-dipole" source. The following spin-density corresponds to two spins of opposite orientation separated by a vector $\vec{a}$ traveling together at velocity $\vec{v}$:

$$\vec{s} = \vec{S}\, \delta^{(3)}(\vec{r} + \vec{a}/2 - \vec{v}t) - \vec{S}\, \delta^{(3)}(\vec{r} - \vec{a}/2 - \vec{v}t). \tag{20}$$

Repeating the same calculation as above, we find

$$\frac{dE_{\text{dipole}}}{dt} \sim -\frac{M^2}{F^2} \int d^3k \frac{(\vec{k} \cdot \vec{S})^2 (\vec{k} \cdot \vec{v}) \sin^2(\vec{k} \cdot \vec{a}/2)}{(M\vec{k} \cdot \vec{v})^2 - k^4}. \tag{21}$$

Again, the integral over the magnitude of k is easy because of the simple poles.

$$\frac{dE_{\text{dipole}}}{dt} \sim -\frac{M^4}{F^2} \int d\Omega\, (\hat{k} \cdot \vec{S})^2 |\hat{k} \cdot \vec{v}|^3 \sin^2 \left(\frac{M(\hat{k} \cdot \vec{v})(\hat{k} \cdot \vec{a})}{2} \right) \tag{22}$$

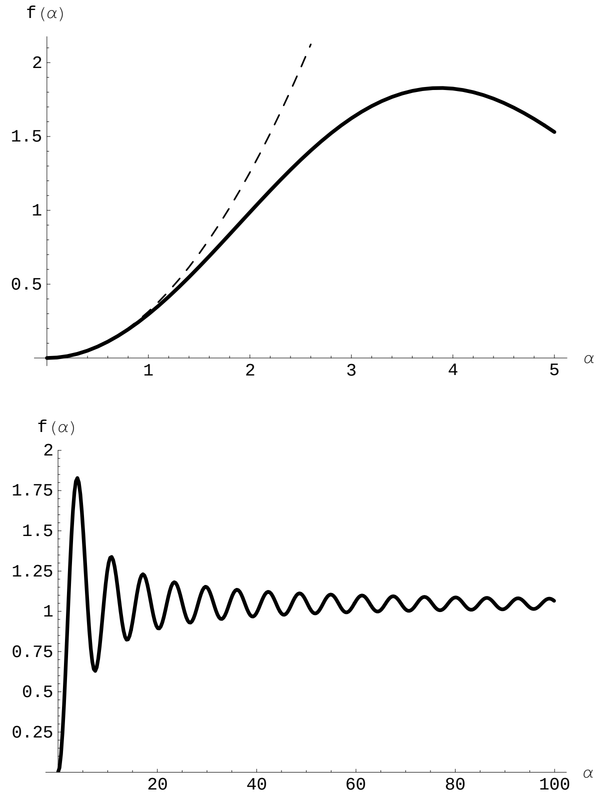

Figure 1: The function $f(\alpha)$ for small and large α. The dashed curve is the best fit parabola near $\alpha = 0$.

To get an idea for what this function looks like, we can go to the special case where $\vec{a}$, $\vec{v}$, and $\vec{S}$ all point in the $\hat{z}$ direction. Introducing the parameter $\alpha = Mva$,

$$\begin{aligned} \frac{dE_{\rm dipole}}{dt} &\sim -\frac{M^4}{F^2} S^2 v^3 \int d\Omega \, (\hat{k}\cdot\hat{z})^2 |\hat{k}\cdot\hat{z}|^3 \sin^2\left(\frac{\alpha}{2}(\hat{k}\cdot\hat{z})(\hat{k}\cdot\hat{z})\right) \\ &\equiv -\frac{M^4}{F^2} S^2 v^3 f(\alpha). \end{aligned} \tag{23}$$

A plot of $f(\alpha)$ appears in Figure 1. We see that for small α, $f(\alpha)$ is quadratic in α. This corresponds to the case that the spacing between the spins is much less than the length scale $1/M$.

$$\frac{dE_{\rm dipole}}{dt} \sim -\frac{M^4}{F^2} S^2 v^5 (Ma)^2 \qquad (Mva \ll 1) \tag{24}$$

When α is large, $f(\alpha)$ asymptotes to a constant value. This corresponds to the case that the spins are far apart compared to $1/M$ such that they can no longer be thoughts of as a spin-dipole and should be treated as individual spins.

$$\frac{dE_{\rm dipole}}{dt} \sim -\frac{M^4}{F^2} S^2 v^3 \qquad (Mva \gg 1) \tag{25}$$

Clearly, any energy dissipation due to ether drag must be very small because we don't observe bodies with spin spontaneously slow down — or rather, speed up in the frame moving with respect to the ether.

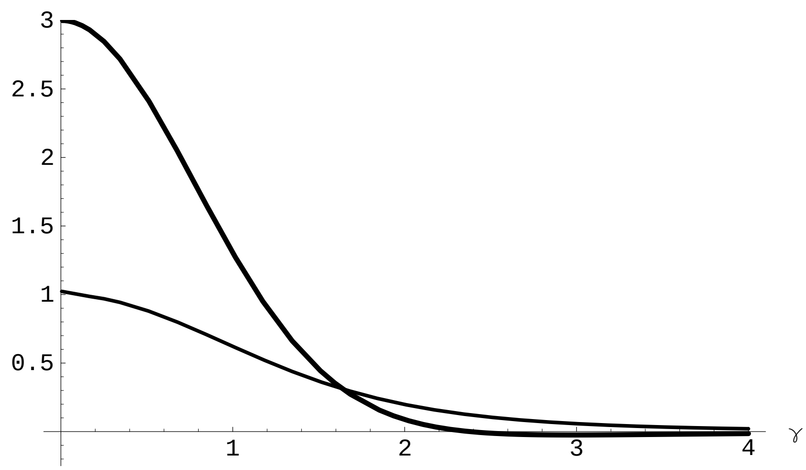

Figure 2: The functions $A(\gamma)$ and $B(\gamma)$ for $\gamma \sim \mathcal{O}(1)$. The top curve is $B(\gamma)$. Note that in the limit $\gamma \to 0$, these functions reproduce the results of equation (19).

To get a sense of it's magnitude, consider the effect of this spin-drag on the earth. The earth has a magnetic dipole moment of $\mu \sim 10^{23}$ A m^2, which corresponds to a net spin of

$$S \sim \frac{\mu}{\mu_B} = 10^{46}, \tag{26}$$

where $\mu_B \sim 10^{-23}$ A m^2 is the Bohr magneton. The velocity of the earth relative to the CMB is $v \sim 10^{-3}$, though it need not be the case that the CMB rest frame is the same as the ether rest frame. From experiments looking at torsion balance tests of direct spin couplings to the earth's velocity, the upper bound on M^2/F is 10^{-25} GeV. In natural units 1 GeV$^{-1} \sim 10^{-25}$ s, so we can calculate that

$$\frac{dE_{\text{earth}}}{dt} \sim \left(\frac{M^2}{F}\right)^2 S^2 v^3 \sim 10^{58} \text{ GeV s}^{-1}. \tag{27}$$

This is a huge energy loss! The mass of the earth is $M_E \sim 10^{51}$ GeV, corresponding to a kinetic energy of

$$E = \frac{1}{2} M_E v^2 \sim 10^{45} \text{ GeV}. \tag{28}$$

By this calculation, the earth would come to rest in the CMB frame in less than a second!

But we've neglected a crucial point: the earth is not a point spin. We need to be more careful and consider the ether drag on finite sources. For example, we can find the energy loss of a Gaussian spin density:

$$\vec{s} = \frac{\vec{S}}{(2\pi R^2)^{3/2}} \exp\left(-\frac{1}{2}\left(\frac{\vec{r} - \vec{v}t}{R}\right)^2\right). \tag{29}$$

Following the exact same logic as above, we find the following expression for the rate of energy dissipation:

$$\frac{dE_{\text{Gaussian spin}}}{dt} = -\frac{M^4}{F^2}\frac{|v|}{96\pi}\left(A(\gamma)|S|^2|v|^2 + B(\gamma)(\vec{S}\cdot\vec{v})^2\right), \tag{30}$$

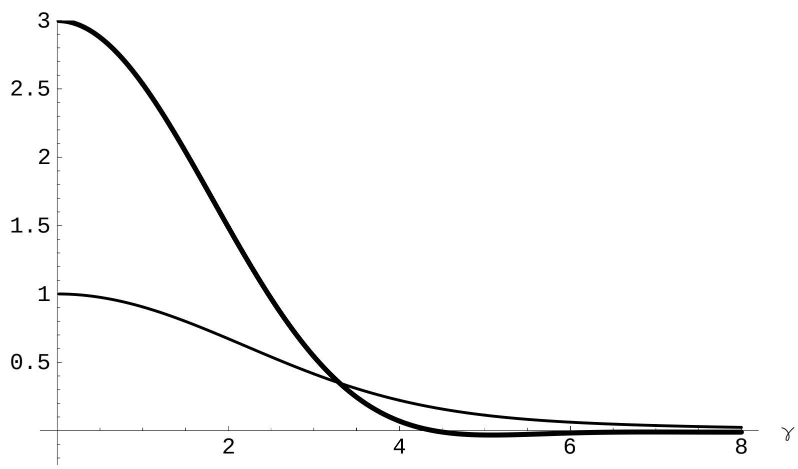

Figure 3: The functions $C(\gamma)$ and $D(\gamma)$ for $\gamma \sim \mathcal{O}(1)$. The top curve is $D(\gamma)$. Note the γ scale difference between this graph and Figure 2.

where $\gamma = MRv$, and

$$A(\gamma) = \frac{6}{\gamma^6}\left((\gamma^2-2)+e^{-\gamma^2}(\gamma^2+2)\right), \qquad B(\gamma) = \frac{6}{\gamma^6}\left((\gamma^2-6)-e^{-\gamma^2}(2\gamma^4+5\gamma^2+6)\right). \tag{31}$$

Plots of $A(\gamma)$ and $B(\gamma)$ for small γ appear in Figure 2. For the earth, R is on the order of 1000 km, and a typical value for M is 1 MeV. This yields a γ parameter of 10^{16}. For large γ the functions $A(\gamma)$ and $B(\gamma)$ behave as

$$A(\gamma) \sim \frac{6}{\gamma^4}, \qquad B(\gamma) \sim -\frac{6}{\gamma^4}. \tag{32}$$

Our revised estimate of the energy loss of the earth is then

$$\frac{dE_{\rm earth}}{dt} \sim \left(\frac{M^2}{F}\right)^2 S^2 v^3 \frac{1}{\gamma^4} \sim 10^{-6}\ {\rm GeV\,s^{-1}}. \tag{33}$$

To see this kind of effect, we would have to wait longer than the age of the solar system!

To check that our answer makes sense, we should verify that the shape of the finite source does not affect the large γ limits. Consider a rectangle function source:

$$\vec{s} = \frac{\vec{S}}{\frac{4}{3}\pi R^3}\begin{cases} 1 & |\vec{r}-\vec{v}t| < R \\ 0 & |\vec{r}-\vec{v}t| > R \end{cases}. \tag{34}$$

This yields the energy dissipation formula,

$$\frac{dE_{\rm rectangle\,spin}}{dt} = -\frac{M^4}{F^2}\frac{|v|}{96\pi}\left(C(\gamma)|S|^2|v|^2 + D(\gamma)(\vec{S}\cdot\vec{v})^2\right). \tag{35}$$

Plots of $C(\gamma)$ and $D(\gamma)$ for small γ appear in Figure 3. They look remarkably similar to the plots in Figure 2 except for a factor of 2 disagreement on the meaning of R. For large γ, the functions behave as

$$C(\gamma) \sim \frac{54\log\gamma}{\gamma^4}, \qquad D(\gamma) \sim -\frac{54\log\gamma}{\gamma^4}, \tag{36}$$

so apart from a $\log\gamma$ factor, we expect that the ether spin drag on finite sources should be reduced by a factor of $\gamma^4 = (MRv)^4$.

Now we see the reason why the ether spin-drag effects are so small. An M of 1 MeV corresponds to a critical radius of 10^{-11} cm, which is on the order of the Compton wavelength of the electron. If we assume that all of the spin of our objects comes from electron spin, then the only way to have a γ of $\mathcal{O}(1)$ is to have a total spin of $\mathcal{O}(1)$. For example, the energy dissipation of an electron is

$$\frac{dE_{\text{electron}}}{dt} = 10^{-25}\ \text{GeV}\,\text{s}^{-1}, \tag{37}$$

which is well beyond the capabilities of current experiments. If we decrease M by 6 orders of magnitude, then the critical radius can enclose 10^{18} "Compton volumes", allowing for a net spin of 10^{18} while still keeping γ of $\mathcal{O}(1)$. In that case dE/dt is on the order of 1 $\text{eV}\,\text{s}^{-1}$ which is certainly measurable. However, for any real spin-polarized material, the spacing between electrons is much larger than the Compton wavelength, and we would never be able to achieve such large spin-densities.

If we were really ambitious, we could calculate the energy dissipation for a rotating spin or an orbiting spin. Unfortunately, any time dependence besides simple velocities makes a nightmare of calculating Fourier transforms, and as of yet, I have been unsuccessful at extracting any useful information about interesting time-dependent spin-densities.

4 Long-Range Spin Dependent Force

Now that we have an understanding of what happens when we have a single spin source, we can now look at interactions involving two spin sources. We will see that the π field can mediate a long-range spin dependent force that falls off much more slowly than typical spin-spin interactions. This raises the interesting possibility of detecting the π field by looking at the force between large magnets, though once again, we will have to contend with suppression factors coming from finite sources.

To start, we will look at the force between point spins due to mediation by a massless spin-0 field φ that has a normal $\omega \sim k$ dispersion relation. Such forces are examined in [4]. In the non-relativistic limit, there is an allowed coupling

$$\mathcal{L}_{\text{int}} = \frac{1}{F}\vec{s}\cdot\vec{\nabla}\varphi. \tag{38}$$

In the Born approximation, the potential between two point spins is the Fourier transform of the propagator times the couplings with $\omega \to 0$.

$$V_\varphi(r) = \frac{1}{F^2}\int \frac{d^3k}{(2\pi)^3}\frac{(-i\vec{k}\cdot\vec{S}_1)(-i\vec{k}\cdot\vec{S}_2)}{k^2}e^{i\vec{k}\cdot\vec{r}} = \frac{-1}{F^2}(\vec{S}_1\cdot\vec{\nabla})(\vec{S}_2\cdot\vec{\nabla})\int\frac{d^3k}{(2\pi)^3}\frac{1}{k^2}e^{i\vec{k}\cdot\vec{r}} \tag{39}$$

The Fourier transform of $1/k^2$ is well-known.

$$V_\varphi(r) = \frac{-1}{F^2}(\vec{S}_1\cdot\vec{\nabla})(\vec{S}_2\cdot\vec{\nabla})\frac{1}{4\pi r} \tag{40}$$

Using the fact that $\partial_i r = x_i/r$,

$$V_\varphi(r) = \frac{1}{4\pi F^2}\frac{(\vec{S}_1\cdot\vec{S}_2) - 3(\vec{S}_1\cdot\hat{r})(\vec{S}_2\cdot\hat{r})}{r^3}. \tag{41}$$

The form of this potential is very similar to the potential between magnetic dipoles in electromagnetism.

What about for the case of the π? The interaction is the same as from equation (6), and with the strange dispersion relation for the π field, the spin-spin potential goes as

$$V_\pi(r) = \frac{-1}{F^2}(\vec{S}_1 \cdot \vec{\nabla})(\vec{S}_2 \cdot \vec{\nabla}) \int \frac{d^3k}{(2\pi)^3} \frac{M^2}{k^4} e^{i\vec{k}\cdot\vec{r}} = \frac{M^2}{F^2}(\vec{S}_1 \cdot \vec{\nabla})(\vec{S}_2 \cdot \vec{\nabla}) \frac{r}{8\pi}. \tag{42}$$

Expanding the derivatives:

$$V_\pi(r) = \frac{M^2}{8\pi F^2} \frac{(\vec{S}_1 \cdot \vec{S}_2) - (\vec{S}_1 \cdot \hat{r})(\vec{S}_2 \cdot \hat{r})}{r}. \tag{43}$$

The novel dispersion relation for π has produced a long range $1/r$ potential between spins! Assuming that M/F is not too small, we might be able to design experiments to measure this force.

Before we get too excited, we have to be careful about two things. One is that for a real experiment we will be dealing with finite sources, and just like the example of Cherenkov radiation, we expect to see some suppression by the size of the sources. But even putting that aside, we need to understand what the Born approximation really means in this context. By taking $\omega \to 0$, we are assuming that $\omega \ll k^2/M$. In position space, this means that our approximation is only valid on time scales

$$t \gg Mr^2. \tag{44}$$

For a normal $\omega \sim k$ dispersion relation, we have to only wait a time $t = r$ for our system to behave "non-relativistically". For the π mediated forces, however, the time to reach steady state is increased by a factor of Mr. For an M of 1 MeV, this factor is $r/(10^{-11}$ cm), or the number of electron Compton wavelengths between the spins. This is a huge number for any macroscopic separation. Thus, in order to understand how the spin-spin force evolves, we should really calculate $V_\pi(r,t)$.

We will start with a spin source at the origin that turns on at $t = 0$:

$$\vec{s} = \vec{S}_1\, \delta^{(3)}(\vec{r})\, \theta(t). \tag{45}$$

Assuming a test spin $\vec{S}_2$ sitting at $\vec{r}$, the expression for $V_\pi(r,t)$ is

$$\begin{aligned} V_\pi(r,t) &= \frac{-1}{F^2}(\vec{S}_1 \cdot \vec{\nabla})(\vec{S}_2 \cdot \vec{\nabla}) \int d^3r_0\, dt_0\, \delta^{(3)}(\vec{r}_0)\, \theta(t_0) \int \frac{d^3k\, dw}{(2\pi)^4} \frac{1}{w^2 - k^4/M^2} e^{i\vec{k}\cdot(\vec{r}-\vec{r}_0)} e^{-iw(t-t_0)} \\ &= \frac{-1}{F^2}(\vec{S}_1 \cdot \vec{\nabla})(\vec{S}_2 \cdot \vec{\nabla}) \int \frac{d^3k}{(2\pi)^3} \frac{M^2}{k^4} \left(1 - \cos(tk^2/M)\right) e^{i\vec{k}\cdot\vec{r}}, \end{aligned} \tag{46}$$

where we have used a pole prescription corresponding to the retarded potential. For large t, the oscillatory part of the integral vanishes, and we recover the result from equation (42). When $t = 0$, the potential is zero, as we would expect because information about $\vec{S}_1$ has not yet reached $\vec{S}_2$. If we had a normal $\omega \sim k$ dispersion relation, then the potential would turn on suddenly when $t = r$. Here, however, there is no Lorentz invariance, so we have no reason to expect a vanishing potential outside the light-cone.

To solve for the potential, we perform the angular k integrals, and then introduce the variables $z = k\sqrt{t/M}$ and $\vec{s} = \vec{r}\sqrt{M/t}$.

$$\begin{aligned} V_\pi(r,t) &= \frac{-M^2}{F^2}(\vec{S}_1 \cdot \vec{\nabla}_s)(\vec{S}_2 \cdot \vec{\nabla}_s)\sqrt{\frac{M}{t}} \int_{-\infty}^{\infty} \frac{dz}{(2\pi)^2} \frac{1}{iz^3} \left(1 - \cos(z^2)\right) \frac{e^{izs}}{s} \\ &\equiv \frac{-M^2}{F^2}\sqrt{\frac{M}{t}}(\vec{S}_1 \cdot \vec{\nabla}_s)(\vec{S}_2 \cdot \vec{\nabla}_s) h(s). \end{aligned} \tag{47}$$

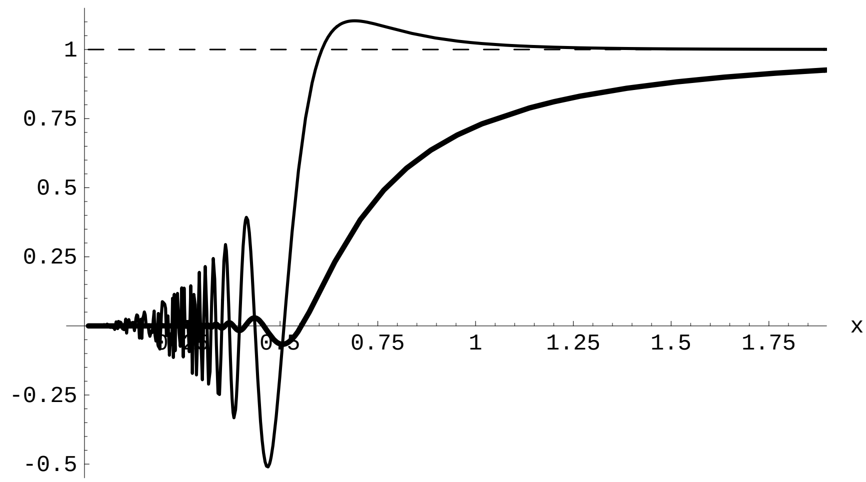

Figure 4: The functions $K(x)$ and $L(x)$ for $x \sim \mathcal{O}(1)$. The top curve is $L(x)$. Note that both functions asymptote to 1 in the large x limit.

Performing the derivatives:

$$V_\pi(r,t) = \frac{M^2}{8\pi F^2} \frac{K(t/Mr^2)(\vec{S}_1 \cdot \vec{S}_2) - L(t/Mr^2)(\vec{S}_1 \cdot \hat{r})(\vec{S}_2 \cdot \hat{r})}{r}, \tag{48}$$

where

$$K(x) = -h'(1/x^2), \qquad L(x) = \frac{1}{x^2} h''(1/x^2) - h'(1/x^2). \tag{49}$$

Plots of these functions appear in Figure 4. We see that the potential does not come to its full value until $t \sim Mr^2$. However, for t small compared to Mr^2, it appears that the potential oscillates between being attractive and repulsive.

One possibility is that by postulating a source that turns on suddenly at $t = 0$, we are introducing transients into the potential. Thus, we would like to smooth out the potential in order to understand the small t behavior and check whether the oscillations are real. Consider the following source:

$$\vec{s} = \vec{S}_1\, \delta^{(3)}(\vec{r}) \begin{cases} 1 & t > 0 \\ 1 + t/T & -T < t < 0 \\ 0 & t < -T \end{cases} . \tag{50}$$

This corresponds to a linear ramping of the source that begins at $t = -T$ and reaches its final value at $t = 0$. Performing the exact same manipulations at before, we find

$$V_\pi(r,t) = \frac{-M^2}{F^2} \sqrt{\frac{M}{t}} (\vec{S}_1 \cdot \vec{\nabla}_s)(\vec{S}_2 \cdot \vec{\nabla}_s) h_{\rm mod}(s, t/T), \tag{51}$$

where $h_{\rm mod}(s,t/T)$ is some new function with explicit time dependence. As a check that the limits work out correctly, we note that $h_{\rm mod}(s,\infty) = h(s)$. We can now easily calculate the new functions $K_{\rm mod}(x, T/Mr^2)$ and $L_{\rm mod}(x, T/Mr^2)$ that would plug into equation (48), where as before $x = t/Mr^2$. Graphs of these functions appear in Figure 5.

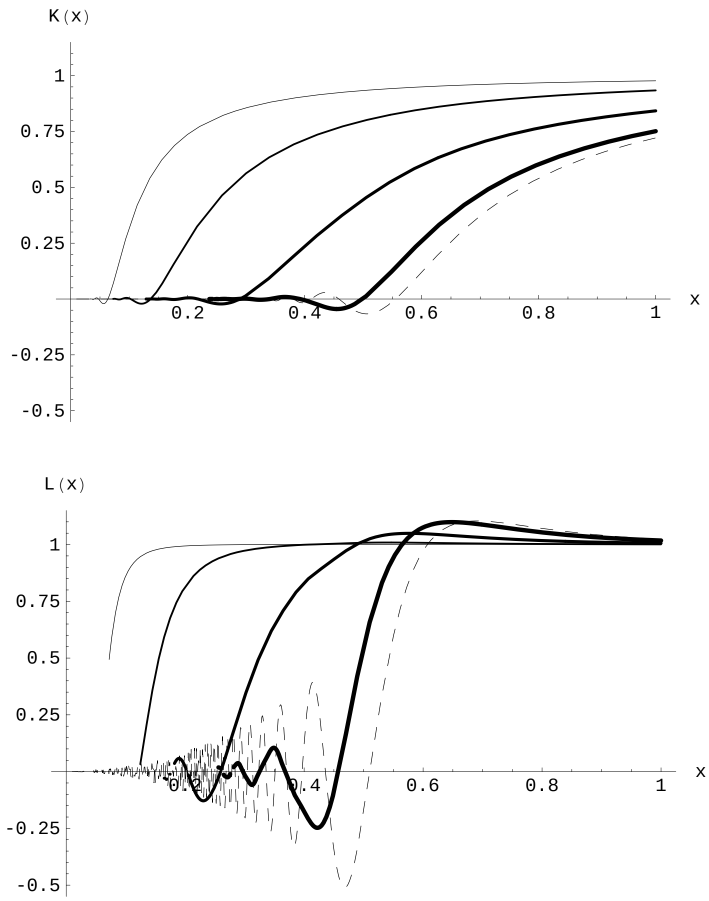

Figure 5: The functions $K_{\rm mod}(x, T/Mr^2)$ and $L_{\rm mod}(x, T/Mr^2)$ for $x \sim \mathcal{O}(1)$. From right to left, the graphs correspond to $T/Mr^2 = 0$ (dashed), .5, 5, 50, 500. The range of x values are limited by numerical precision. For $T \to \infty$, the potential is 1 for all x.

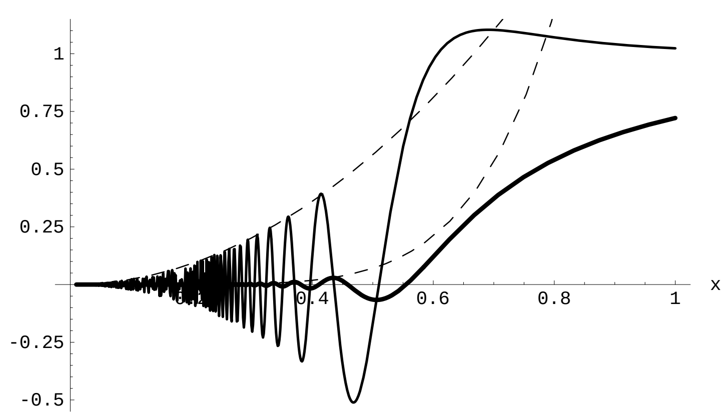

Figure 6: The functions $K(x)$ and $L(x)$ for $x \sim \mathcal{O}(1)$ with dashed lines corresponding to the small x envelopes $|K(x)| \sim 4.5x^6$ and $|L(x)| \sim 2.3x^2$.

We see that the oscillatory behavior is robust to changes in T. As the ratio of T to Mr^2 increases, the amplitude of the modulations decreases and the onset of the full potential comes sooner, but there is still some small oscillatory behavior. As seen in Figure 6, in the $T \to 0$ limit the oscillations have amplitude

$$|K(x)| \sim x^6, \qquad |L(x)| \sim x^2. \tag{52}$$

Because $x = t/Mr^2$, it appears that for early times, the $K(x)$ piece acts as a $1/r^{13}$ oscillatory potential and the $L(x)$ piece acts like a $1/r^5$ oscillatory potential until both pieces settle down to a $1/r$ potential at $t \sim Mr^2$.

Now we would like to understand any suppression of the potential coming from finite sources. Ignoring time dependence, we can use a rectangle source:

$$\vec{s} = \frac{\vec{S}}{\frac{4}{3}\pi R^3} \begin{cases} 1 & |\vec{r}| < R \\ 0 & |\vec{r}| > R \end{cases} . \tag{53}$$

If we have a test spin $\vec{S}_2$ at $\vec{r}$, the expression for V_π is (after Fourier transforming $\vec{s}$):

$$V_\pi(r) = \frac{-1}{F^2}(\vec{S}_1 \cdot \vec{\nabla})(\vec{S}_2 \cdot \vec{\nabla}) \int \frac{d^3k}{(2\pi)^3} \frac{M^2}{k^4} \frac{3(\sin kR - kR\cos kR)}{(kR)^3} e^{i\vec{k}\cdot\vec{r}}. \tag{54}$$

We only care about the potential for $r > R$ (*i.e.* outside the source). Performing the integral and doing the derivatives:

$$V_\pi(r) = \frac{M^2}{8\pi F^2} \frac{P(R/r)(\vec{S}_1 \cdot \vec{S}_2) - Q(R/r)(\vec{S}_1 \cdot \hat{r})(\vec{S}_2 \cdot \hat{r})}{r}, \tag{55}$$

where

$$P(R/r) = 1 - \frac{R^2}{5r^2}, \qquad Q(R/r) = 1 - \frac{3R^2}{5r^2}. \tag{56}$$

So although there is a suppression when the test spin is very close to the source, for separations large compared to the size of the sources, we can ignore the effects of finite sources. Similarly, if we were conducting an actual experiment with magnets, we need not worry about bringing the magnets too close together, because by varying r, we could isolate the $1/r$ dependence coming from our π field from the $1/r^3$ dependence that we could ascribe to a hypothetical φ field. We can see from equation (41) that even the factor of 3 works out.

All of our calculations have been done in the ether rest frame. At this point, we should check the potential for spins moving with various velocities relative to the ether to see whether there is any interesting velocity dependence. In particular, experiments on the earth with magnets fixed to the surface of the earth would be described by sources moving together with a slowly varying velocity v. We might expect that if the source and test spin are traveling fast with respect to the ether, then the π waves will not be able to "keep up", and the spin-spin potential will be suppressed. What we will actually find is far more interesting.

Consider a moving source:

$$\vec{s}_1 = \vec{S}_1 \delta^{(3)}(\vec{r} - \vec{v}t). \tag{57}$$

We want to look at the co-moving potential, namely the potential between $\vec{S}_1$ and some test spin $\vec{S}_2$ that is moving at the same velocity as $\vec{S}_1$. Following a similar logic to our previous calculations, we find

$$V(r) = \frac{M^2}{F^2}(\vec{S}_1 \cdot \vec{\nabla})(\vec{S}_2 \cdot \vec{\nabla}) \int \frac{d^3k}{(2\pi)^3} \frac{e^{i\vec{k}\cdot\vec{r}}}{(M\vec{k}\cdot\vec{v})^2 - k^4} \equiv \frac{M^2}{8\pi F^2}(\vec{S}_1 \cdot \vec{\nabla})(\vec{S}_2 \cdot \vec{\nabla}) f(r, Mv, \theta_v), \tag{58}$$

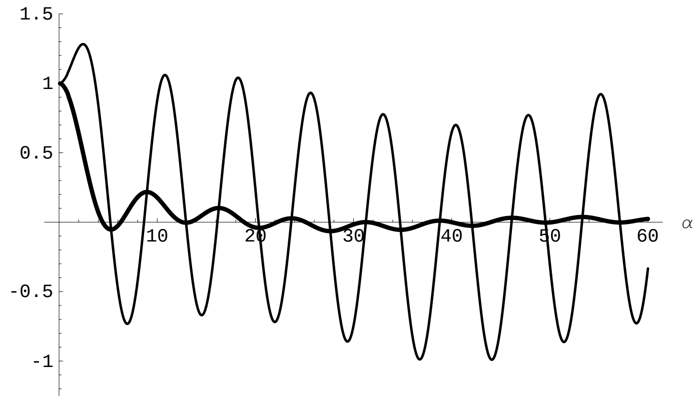

Figure 7: The functions $A(\alpha, \pi/4)$ and $B(\alpha, \pi/4)$. The top function is $B(\alpha, \pi/4)$. Note that in the limit $\alpha = 0$, we recover the zero comoving velocity behavior.

where $\cos\theta_v = \hat{r} \cdot \hat{v}$, and

$$f(r, Mv, \theta_v) = 8\pi \int \frac{dk\, d\Omega\, k^2}{(2\pi)^3} \frac{e^{ik\hat{k}\cdot\vec{r}}}{k^2 \left((M\hat{k}\cdot\vec{v})^2 - k^2\right)}. \tag{59}$$

To evaluate this integral, we will do the integral over the ranges $k \in (-\infty, \infty)$, $k_\theta \in (0, \pi/2)$, and $k_\phi \in (0, 2\pi)$. The pole prescription to find the Fourier transform is to split each pole into two pieces, one in the upper half plane and one in the lower half plane. By our choice of integration ranges, we can safely close the k contour in the upper half plane. The expression for f becomes:

$$f(r, Mv, \theta_v) = \frac{8\pi}{2} \int \frac{d\Omega}{(2\pi)^2} \frac{\sin\left(Mrv(\hat{k}\cdot\hat{r})(\hat{k}\cdot\hat{v})\right)}{Mv\hat{k}\cdot\hat{v}}. \tag{60}$$

Note that in limit $v \to 0$, we recover $f(r) = r$, as from equation (42). Applying the derivatives to f, the potential looks like

$$V(r) = \frac{M^2}{8\pi F^2} \frac{A(\alpha, \theta_v)(\vec{S}_1 \cdot \vec{S}_2) - B(\alpha, \theta_v)(\vec{S}_1 \cdot \hat{r})(\vec{S}_2 \cdot \hat{r})}{r}, \tag{61}$$

where $\alpha = Mrv$ and

$$A(\alpha, \theta_v) = \frac{d}{dr} f(r, Mv, \theta_v), \qquad B(\alpha, \theta_v) = \frac{d}{dr} f(r, Mv, \theta_v) - r\frac{d^2}{dr^2} f(r, Mv, \theta_v). \tag{62}$$

To get an idea of what the functions A and B look like, we can evaluate them in certain limits. For example, when the velocity vector is parallel to the spin displacement,

$$A(\alpha, 0) = \frac{\sin\alpha}{\alpha}, \qquad B(\alpha, 0) = \frac{2\sin\alpha}{\alpha} - \cos\alpha. \tag{63}$$

Similarly, when the velocity vector is perpendicular to the spin displacement,

$$A(\alpha, \pi/2) = \frac{2}{\alpha}\sin\left(\frac{\alpha}{2}\right), \qquad B(\alpha, \pi/2) = \frac{4}{\alpha}\sin\left(\frac{\alpha}{2}\right) - \cos\left(\frac{\alpha}{2}\right). \tag{64}$$

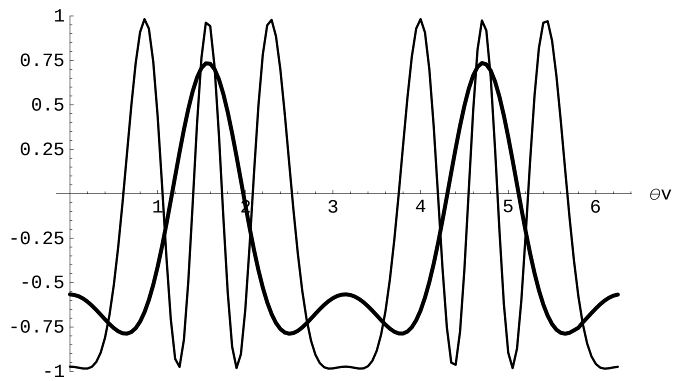

Figure 8: The functions $B(7, \theta_v)$ and $B(19, \theta_v)$. The top function is $B(19, \theta_v)$.

In general, for large α, the functions A and B are bounded by

$$|A(\alpha, \theta_v)| \leq \frac{2}{\alpha}, \qquad |B(\alpha, \theta_v)| \leq 1, \tag{65}$$

so while the A component dies away with increasing α, the B component survives at all distances regardless of how large α is. What is bizarre about these functions are their oscillatory behavior. For example, in Figure 7 we see A and B for $\theta_v = \pi/4$. As α varies, the potential switches between being attractive and repulsive, in much the same way as the early time behavior of equation (51). Similarly, if we fix α and vary θ_v, we see similar kinds of oscillations, as in Figure 8. The experimental implications are not quite clear, but it is encouraging that we do not see the huge comoving velocity suppression that we might naively expect.

5 Possible Breakdown Near Large Sources

As a check that our framework makes sense, we should verify that introducing large sources does not affect the validity of our effective field theory. In particular, if the coefficient of the source term

$$\mathcal{L}_{\text{int}} = \frac{1}{F} \vec{s} \cdot \vec{\nabla} \pi \tag{66}$$

is large, then we can't ignore the back reaction of the π field on the source $\vec{s}$. Similarly, in order to claim that the π fields don't become strongly coupled and thereby violate unitarity, we need to check that $\vec{\nabla}\pi$ is small compared to the scale M^2. It will turn out that both of these constraints will give the same bounds on the sizes of allowed sources.

Roughly speaking, the source term becomes large when

$$\frac{S}{FR} \sim 1, \tag{67}$$

where S is the total spin of the source, and R is a typical length scale associated with the source. (We've used that $\vec{\nabla} \sim 1/R$.) If F is some very large scale such as the Planck scale, then R has to be small

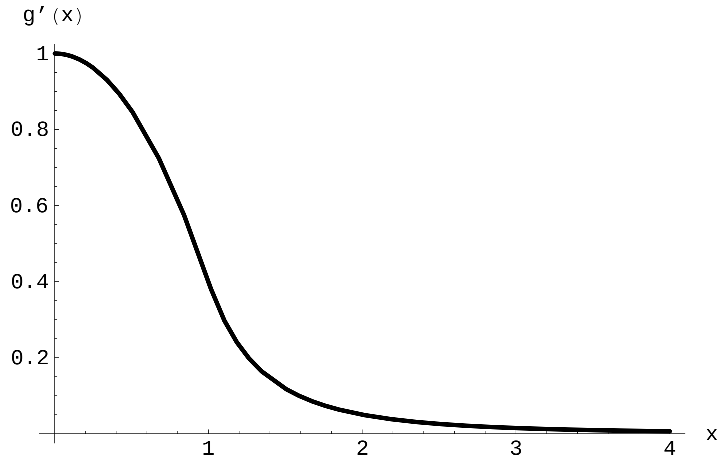

Figure 9: The function $g'(x)$ for x near 1.

compared to this scale for there to be a danger. But even for an electron, $R \gg 1/F$, so we are certainly justified in ignoring the back reaction of the π field on fermion fields.

What about for large sources at rest relative to the ether? Again consider the rectangle source

$$\vec{s} = \frac{\vec{S}}{\frac{4}{3}\pi R^3} \begin{cases} 1 & |\vec{r}| < R \\ 0 & |\vec{r}| > R \end{cases} . \tag{68}$$

We want to calculate $\vec{\nabla}\pi$ for this source. Again using Green functions,

$$\pi(\vec{r}) \sim \frac{M^2}{F} \int d^3k \, \frac{\vec{k}\cdot\vec{S}}{k^4} \frac{\sin kR - kR\cos kR}{(kR)^3} e^{i\vec{k}\cdot\vec{r}} \sim \frac{M^2 \hat{r}\cdot\vec{S}}{FR} \, g\Big(\frac{r}{R}\Big) , \tag{69}$$

where $g(x)$ is some unenlightening function. Ignoring angular dependence (which turns out to only decrease the magnitude of the gradient), the gradient of π is

$$\nabla\pi(r) \sim \frac{M^2 S}{FR} \, g'\Big(\frac{r}{R}\Big) . \tag{70}$$

A plot of $g'(x)$ appears in Figure 9. We see that it is well behaved at all values of r/R. Our effective theory will break down when $\vec{\nabla}\pi \sim M^2$, and this occurs when $S/FR \sim 1$, the same result we found in equation (67).

6 Effect of Background Perturbations

Our analysis assumed that $\langle\phi\rangle = M^2 t$ was a good background for the π field. While this assumption is good when the sources of ϕ are small, gravitational effect can distort the ϕ profile and add spacial inhomogeneities. While these inhomogeneities are not fully understood yet, we will show that as long as the typical length scale of inhomogeneities is large compared to the size of our experiments, then we can understand the effect of spacial inhomogeneities simply as a redefinition of the local velocity of the ether "wind".

Consider expanding around the background $\langle\phi\rangle = M^2 t + \epsilon(\vec{x})$, where $\epsilon(\vec{x})$ is some spacial perturbation. To find the quadratic piece of the Lagrangian for the π field in the canonical ghost language, we expand the leading order ghost Lagrangian

$$\mathcal{L}_{\text{ghost}} = \frac{(\langle\partial_\mu\phi\partial^\mu\phi\rangle - \partial_\mu\phi\partial^\mu\phi)^2}{8M^4} - \frac{(\langle\Box\phi\rangle - \Box\phi)^2}{2M^2} + \ldots \tag{71}$$

about the vev of ϕ. Going to canonical normalization for the π field, the quadratic piece of the Lagrangian in the non-relativistic limit is

$$\mathcal{L}_{\text{quad}} = \frac{1}{2}\left(\dot{\pi} - \vec{\nabla}\epsilon \cdot \vec{\nabla}\pi\right)^2 - \frac{\left(\nabla^2\pi\right)^2}{2M^2}. \tag{72}$$

At first this seems like we have modified the π propagator, but we can do a (non-relativistic) Galilean coordinate transformation, assuming that the gradient of ϵ does not vary much on a local coordinate patch:

$$\vec{x} \to \vec{x} + (\vec{\nabla}\epsilon)t, \qquad t \to t. \tag{73}$$

Under this coordinate transformation,

$$\frac{\partial}{\partial\vec{x}} \to \frac{\partial}{\partial\vec{x}}, \qquad \frac{\partial}{\partial t} \to \frac{\partial}{\partial t} + \vec{\nabla}\epsilon \cdot \frac{\partial}{\partial\vec{x}}, \tag{74}$$

so we see readily that local inhomogeneities in the ϕ background can be accounted for by a simple "boost" to the local ether "rest frame". Because we have carried out all of our analyses for a generic velocity, our arguments will go through unchanged, assuming that ϕ does not vary much over the typical length scale of any experiment.

7 Outlook

Using the language of effective field theory, we have seen interesting Lorentz violating effects coming from the interaction of Standard Model fermions with the Goldstone boson π associated with spontaneous time diffeomorphism breaking. Though the particular couplings to fermion spin-density can be removed by assuming a $\phi \to -\phi$ symmetry, other couplings to 3-vector densities will be generated through graviton loops, and a similar analysis will hold in those cases. In particular, we expect further examples of Cherenkov-like radiation, as well as forces between sources of 3-vector currents. From our study of finite sources, we expect the Cherenkov effects to be suppressed by some power of MR, in addition to suppression by the Planck scale. And we expect a bizarre velocity dependence in the long-range potential between 3-vector sources.

Because couplings between the π sector and the Standard Model generically generate Lorentz-violations, it is imperative that we catalog all possible interactions between the π field and Standard Model fields so we understand exactly where all Lorentz-violating effects might show up. Our task is made somewhat easier because the scale of spontaneous time diffeomorphism breaking should be around or less than 1 MeV, a scale at which the dominant degrees of freedom are just electrons and photons. In effect, we need only consider Lorentz violating effects in QED, and the non-dynamical interactions are classified in [5]. Our goal is to augment the catalog of non-dynamical interactions with dynamical interactions coming from π physics.

References

[1] N. Arkani-Hamed, H.-C. Cheng, M. A. Luty, and S. Mukohyama. *Ghost Condensation and a Consistent Infrared Modification of Gravity*. hep-th/0312099.

[2] J. Thaler. *Spontaneous Time Diffeomorphism Breaking*. http://www.jthaler.net/physics/notes/TimeDiffeoBreak.pdf.

[3] Peskin and Schroeder, Sec. 3.5, p. 60.

[4] J. E. Moody and F. Wilczek. *New macroscopic forces?* Phys. Rev. D **30**, 130 (1984).

[5] D. Colladay and V. A. Kostelecký. *Lorentz-Violating Extension of the Standard Model*. hep-ph/9809521.